

## Soil erosion risk assessment of the Keiskamma catchment, South Africa using GIS and remote sensing

Paidamwoyo Mhangara · Vincent Kakembo ·  
Kyoung Jae Lim

Received: 18 August 2010 / Accepted: 2 July 2011 / Published online: 21 July 2011  
© Springer-Verlag 2011

**Abstract** This paper examines the soil loss spatial patterns in the Keiskamma catchment using the GIS-based Sediment Assessment Tool for Effective Erosion Control (SATEEC) to assess the soil erosion risk of the catchment. SATEEC estimates soil loss and sediment yield within river catchments using the Revised Universal Soil Loss Equation (RUSLE) and a spatially distributed sediment delivery ratio. Vegetation cover in protected areas has a significant effect in curtailing soil loss. The effect of rainfall was noted as two pronged, higher rainfall amounts received in the escarpment promote vegetation growth and vigour in the Amatole mountain range which in turn positively provides a protective cover to shield the soil from soil loss. The negative aspect of high rainfall is that it increases the rainfall erosivity. The Keiskamma catchment is predisposed to excessive rates of soil loss due to high soil erodibility, steep slopes, poor conservation practices and low vegetation cover. This soil erosion risk assessment shows that 35% of the catchment is prone to high to extremely high soil losses higher than  $25 \text{ ton ha}^{-1} \text{ year}^{-1}$  whilst 65% still experience very low to moderate levels of soil loss of less than  $25 \text{ ton ha}^{-1} \text{ year}^{-1}$ . Object based classification highlighted the occurrence of enriched valley infill which flourishes in sediment laden ephemeral stream channels. This occurrence increases gully erosion due to overgrazing within ephemeral stream channels. Measures

to curb further degradation in the catchment should thrive to strengthen the role of local institutions in controlling conservation practice.

**Keywords** Soil erosion · RUSLE · SATEEC GIS · Remote sensing

### Introduction

Soil erosion by water is a major environmental problem that threatens the ecological function of terrestrial and aquatic systems worldwide (Olderman 1994; Nyakatawa et al. 2001). It is estimated that 85% of global land degradation is associated with soil erosion and close to  $5 \text{ Mg ha}^{-1} \text{ year}^{-1}$  of productive topsoil is lost to lakes and oceans in Africa (Olderman et al. 1990; Angima et al. 2003). Flügel et al. (2003) predict that soil erosion will become more severe in Southern Africa due to population increases and climatic changes. More than 70% of South Africa is affected by soil erosion of varying intensities (Garland et al. 2000; Le Roux et al. 2008). Le Roux et al. (2008) highlight that the Eastern Cape Province has one of the highest erosion potentials in South Africa.

Soil erosion is a natural process and relates to the entrainment and transportation of earth materials across a given surface. Soil loss is defined as the amount of material that is actually removed from a particular slope (Renard et al. 1997); and is one of the major indicators of environmental degradation. The negative effects caused by soil erosion on soil degradation, hydrological systems, agriculture, water quality and the environment in general have long been established and the impacts of soil erosion continue to pose severe threats to human sustenance (Lal 1998). The impacts of soil erosion include loss of fertile

P. Mhangara (✉) · V. Kakembo  
Department of Geosciences, Nelson Mandela Metropolitan  
University, Port Elizabeth, PO Box 77000, South Africa  
e-mail: paidamwoyom@yahoo.com;  
s207049977@live.nmmu.ac.za

K. J. Lim  
Department of Regional Infrastructure Engineering,  
Kangwon National University, Kangwon, Chuncheon, Korea

topsoil, decline of soil productivity and reduction in water quality in river networks. Reservoir sedimentation is one of the direct impacts of soil erosion that exacerbates water management problems in Southern Africa (Flügel et al. 2003). The economic and environmental impacts of accelerated soil erosion are difficult to quantify because of its extent, magnitude, rate and complexity of the processes related to it (Lal 1994).

Timely and accurate estimation of soil loss or evaluation of soil erosion risk is now regarded as an issue of high priority. Many models have been developed to estimate soil loss (Wischmeier and Smith 1978; Nearing et al. 1989; Lim et al. 2005). Among them, the Universal Soil Loss Equation (USLE) (Wischmeier and Smith 1978), Soil and Water Assessment Tool (SWAT) (Arnold et al. 1998), Soil Erosion Model (EUROSEM) (Morgan et al. 1998) and Water Erosion Prediction Project (WEPP) (Flanagan and Nearing 1995) have been widely used. The USLE has been used successfully to estimate soil erosion potential for nearly 40 years (Dennis and Rorke 1999; Kinnell 2000). Process-based erosion models have limited use due to intensive data and computation requirements. The Revised Universal Soil Loss Equation (RUSLE) was developed on the basis of substantial modifications of the USLE and its database to more accurately estimate rainfall erosivity ( $R$ ), soil erodibility ( $K$ ), land cover management ( $C$ ), conservation practice factor ( $P$ ) factors, and soil erosion (Renard et al. 1991). The RUSLE includes the analysis of data that was not previously included in the USLE, and an update of the theory describing hydrologic and erosion processes. Renard et al. (1994) provide a detailed summary of the differences between USLE and RUSLE. Prominent modifications include corrections of the  $R$  factor, new equations based on the ratio of rill to interrill erosion that accommodate complex aspects  $LS$  factor and the implementation of new subfactors for calculating the  $C$  factor and the new  $P$  factor (Renard et al. 1991). Notwithstanding these modifications, the RUSLE model has retained the same fundamental structure as the USLE (Renard et al. 1994).

The RUSLE model has been used extensively in predicting soil loss around the world. Wischmeier and Smith (1978) originally developed the USLE for soil erosion estimation in croplands on gently sloping topography. While the RUSLE model has gained acceptance for use at river catchment and regional scales (Fu et al. 2005; Onori et al. 2006; Le Roux et al. 2008), USLE and RUSLE were initially developed to estimate soil erosion at small hill-slope and plot scale (Wischmeier and Smith 1978). The SATEEC model can be used for soil erosion risk assessment at watershed scale because of the sediment delivery ratio (SDR) module integrated in it (Lim et al. 2005; Park et al. 2010). The SDR is defined as the ratio of sediment yield to the total surface erosion as affected by catchment

topography, land cover, sediment sources, transport system and texture of eroded material (Walling 1988; Bhattarai and Dutta 2007). The concept of SDR encapsulated within the RUSLE based SATEEC model is an important paradigm at catchment scale since significant sediment deposition occurs within the catchment before it reaches the catchment outlet (Bhattarai and Dutta 2007). The SATEEC model is thus a substantial improvement of the RUSLE model since it incorporates spatially disturbed sediment delivery ratios to compute soil loss from rill and interrill erosion.

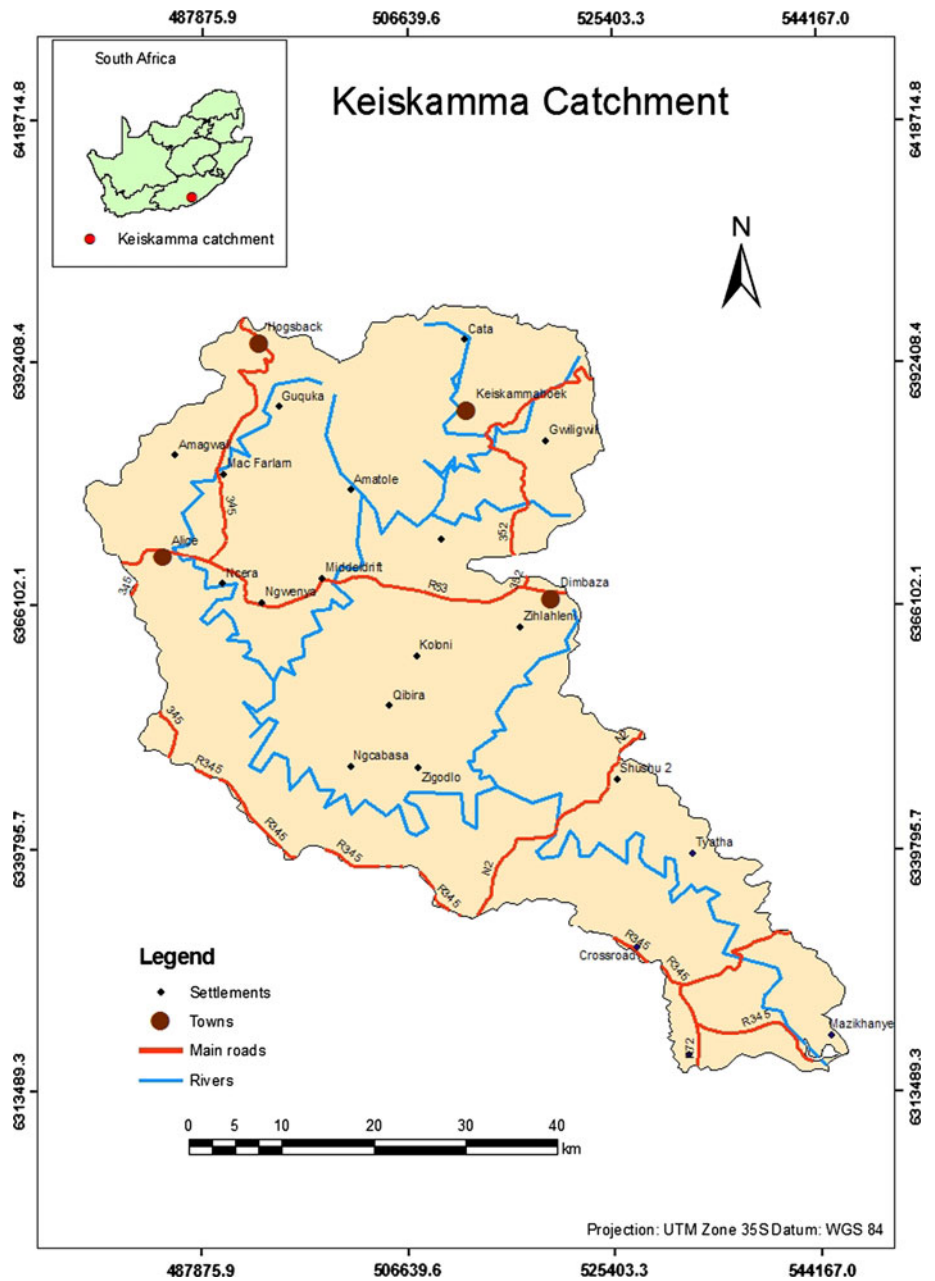
Mapping soil erosion in large areas using traditional methods is a difficult task. The use of remote sensing in conjunction with GIS techniques makes soil erosion estimation and its spatial distribution attainable at a higher accuracy and lower cost (Wang et al. 2003). The integrated application of remote sensing, GIS and RUSLE provides the potential to estimate soil erosion loss on a cell-by-cell basis (Millward and Mersey 1999). Soil erosion risk was assessed successfully using RUSLE by Boggs et al. (2001) using a Digital Elevation Model (DEM) and land-unit maps. Related studies also successfully applied the RUSLE model to soil erosion risk mapping using remote sensing and GIS techniques (Bartsch et al. 2002; Wang et al. 2003). The RUSLE parameters can be altered significantly by human activities. The  $C$  factor can be changed by deforestation; the  $P$  factor can be transformed by shifting community environmental practices and the  $L$  factor by changing the dimensions of the fields.

Sediment analysis provides an integrated view of sediment sources, transfers, sinks and outputs of a drainage basin, and draws together the many aspects of erosion, sediment mobilization, transport, storage and yield. According to a review by Le Roux et al. (2007) of erosion assessment projects conducted in South Africa, the evaluation of soil erosion risk within the context of environmental degradation has not attracted sufficient scientific attention in the Eastern Cape Province of South Africa. In particular, soil erosion modelling that integrates sediment delivery ratios in GIS has not been undertaken. Furthermore, while the use of remote sensing has gained attention in mapping soil erosion (Märker et al. 2001; Flügel et al. 2003; Taruvinga 2009), the application of object oriented classification techniques to map soil erosion phenomena has not yet been explored.

Thus, the objectives of this study are:

1. To determine the spatial patterns of soil loss in the Keiskamma catchment using a GIS based RUSLE model that integrates sediment delivery ratios to assess the environmental health status of the catchment.
2. To map gully erosion surfaces and valley infill in ephemeral stream channels using object oriented

**Fig. 1** Map showing the location of the Keiskamma catchment in South Africa



classification as a means of demonstrating the major sediment transfer processes operating in the Keiskamma catchment. Sediments are transferred mostly from rills and gullies (sediment sources) into ephemeral stream channels which act as sediment sinks.

**Study area**

The Keiskamma catchment is located in the Eastern Cape Province of South Africa, and falls within the greater Amatola catchment (Fig. 1). It is largely constituted by

nucleated communal settlements designed during the betterment programme of the apartheid era in the 1960s and 1970s. Small towns such as Keiskamma, Alice, Hogsback and Dimbaza are also found within the catchment. Forest plantations are found along the Amatola mountain range. The catchment is characterized by three topographic zones which are the escarpment zone or mountain highlands, the coastal plateau and the coastal belt (DWAf 2004). The coastal belt extends into the catchment for approximately 20 km. The coastal plateau covers most of the catchment with altitudes ranging from 600 to 900 m above mean sea level and reaches the base of the Amatola mountain range.

The escarpment zone has elevations of up to 1,938 m and is located between the catchment divide and the coastal plateau. The incised Keiskamma River valley bisects the plateau and coastal belt.

The escarpment areas are characterized by dense bush called the valley thicket in the river valleys and indigenous forest in the mountain zone. Protected areas in the catchment include Middledrift gamepark, the Hogsback and Keiskamma Nature Reserve along the Amatola mountain range and the forest plantation areas. Coastal grasslands, savannah (thornveld or sourveld) vegetation constitute the coastal belt and coastal plateau. Black and silver wattle invasions also characterize some parts of the catchment. The main Keiskamma river has its headwaters in the Amatola mountains above Keiskammahoek and winds eastwards for 263 km to drain into the Indian Ocean at the Keiskamma estuary (33°17'S; 27°29'E) located at Hamburg midway between East London in the north and Port Alfred in the south. The Keiskamma catchment is 2,745 km<sup>2</sup> big. The Tyume River is the main tributary of the Keiskamma River.

Today the Keiskamma catchment faces severe threat of land degradation as result of variety of factors such as overgrazing by cattle, sheep and goat, deforestation due to wood harvesting, alien plant invasions in post disturbed areas. Highly erodible soils derived from shales and mudstone are prevalent throughout most parts of the catchment (D'Huyvetter 1985). Rainfalls amounts experienced in the catchment range as high as 1,600 mm per annum in the escarpment region and below 300 mm in the some parts of the catchment, topography seems to have a profound influence in rainfall distribution in the catchment (Tanga 1992).

## Methods

This study applied the RUSLE model in the GIS-based Sediment Assessment Tool for Effective Erosion Control (SATEEC) to estimate soil loss and sediment yield for any location within the Keiskamma catchment using RUSLE input data and the spatially distributed sediment delivery ratio. SATEEC is an ArcView extension developed by Lim et al. (2005), which is an effective tool to estimate soil loss and sediment yield.

The RUSLE equation (metric) is defined as:

$$A = R \times K \times L \times S \times C \times P \quad (1)$$

where  $A$  annual soil loss (ton ha<sup>-1</sup> year<sup>-1</sup>),  $R$  rainfall erosivity factor (MJ mmha<sup>-1</sup> year<sup>-1</sup>),  $K$  = soil erodability factor (ton h MJ<sup>-1</sup> mm<sup>-1</sup>),  $L$  slope length factor,  $S$  slope steepness factor,  $C$  cover-management factor, and  $P$  supporting practices (Renard et al. 1997).

## Parameters used for soil erosion assessment

The derivations of the RUSLE parameters required as inputs in the SATEEC GIS System to predict the average annual rate of soil loss are discussed in this section. The key factors that are explored are: rainfall-runoff erosivity factor ( $R$ ), soil erodibility factor ( $K$ ), slope-length and slope steepness ( $LS$ ) factors and cover management factor ( $C$ ). All datasets were projected to UTM WGS 84 projection system and resampled to a grid resolution of 20 m.

### Rainfall-runoff erosivity factor ( $R$ )

Rainfall is a driver of soil erosion processes and its effect is accounted for by the rainfall-runoff erosivity factor ( $R$ ) in the RUSLE equation. The  $R$ -factor accounts for the effect of raindrop impact and also shows the amount and rate of runoff associated with precipitation events. The  $R$  factor is computed as total storm energy ( $E$ ) time the maximum 30-min intensity ( $I_{30}$ ), or EI, and is expressed as the rainfall erosion index (Renard et al. 1997). Lack of continuous pluviograph data relating to rainfall intensity motivated the application of the equation established by Wischmeier and Smith (1978) to derive the  $R$  factor. Climate data for the Keiskamma catchment were obtained from the Water Research Commission (WRC 1995a). Rainfall related data for the catchment spanned a period of 52 years. Rainfall data were imported into ArcView since all the weather stations had co-ordinates. Annual and monthly rainfall data for the Keiskamma catchment obtained over 52 years were used to calculate the  $R$ -factor in this study. The equation below developed by Wischmeier and Smith (1978) was used in the computation.

$$R = \sum_{i=1}^{12} 1.735 \times 10^{(1.5 \log \frac{p_i^2}{p} - 0.8188)} \quad (2)$$

where  $p_i$  is the monthly amounts of precipitation and  $p$  is annual precipitation. The annual summation of  $p_i^2/p$  is called the Fournier equation. In recent years, a number of interpolation methods have been developed in GIS that are suitable to model rainfall erosivity. Interpolation methods available in most GIS software include the inverse distance weighting (IDW), kriging, spline polynomial trend, and natural neighbour methods. In this study, the rainfall erosivity values for the different stations were used to interpolate a rainfall erosivity surface using the IDW technique available in ArcGIS 9.0. The IDW interpolation method was selected because rainfall erosivity sample points are weighted during interpolation such that the influence of rainfall erosivity is most significant at the measured point and decreases as distance increases away from the point.

Soil erodibility factor (*K*)

Soil erodibility factor (*K*) in the RUSLE equation is an empirical measure which expresses the inherent susceptibility of a soil to water erosion as determined by intrinsic soil properties. The *K* factor is rated on a scale from 0 to 1, with 0 indicating soils with the least susceptibility to erosion and whilst 1 indicates soils which are highly susceptible to soil erosion by water. The factor is defined as the rate of soil loss per rainfall erosion index unit as measured on a standard plot.

A digital soil classification coverage captured from a soil map by the Water Research Commission was supplied by the Department of Water Affairs and Forestry for integration into the USLE computation (WRC 1995b). Highly erodible soils derived from shales and mudstones are prevalent throughout the catchment. Soil forms present in the catchment include the Glenrosa, Misaphs, Oakleaf, Shortland, Hutton, Arcadia and Valrivier (Weaver 1991). These soil forms falls within the lithic, oxidic, cumulic and melanic soil groups. Small amounts of stable and well structured soils derived from dolerite are also found in the upper part of the catchment (D’Huyvetter 1985). The topsoil is highly vulnerable to erosion due to the dispersive character of the soils inherited from the underlying geology and is further exacerbated by the removal of vegetation. The Misaphs and Glenrosa soil forms of the lithic soil group and Hutton soils of the oxidic soil group are, however, the most widespread soil types and were used to obtain a general characterization of the soil erodibilities in this study. These soils are predominately sandy loams and sandy clay loams.

Fieldwork was conducted to collect soil samples to determine the particle size distribution where the Misaph, Hutton and Glenrosa soils are the dominant soil types. A total of 12 random samples were collected for each area with the dominant soil type; a soil map was used to determine the spatial distribution of the soil forms in the field. The co-ordinates for the soil sampling locations were collected using a Global Position System (GPS). Soil erodibility was calculated using Eq. 3 developed by Wischmeier and Smith (1978). The equation effectively describes soil erodibility as a function of the complex interaction between sand, silt, and clay fractions in the soil and other factors such as organic matter, soil structure and profile permeability class. In general, soils become less erodible with decrease in silt content, regardless of corresponding increases in the sand or clay fraction (Wischmeier and Smith 1978).

$$K = [(2.1 \times 10^{-4}(12 - OM)M^{1.14} + 3.25(S - 2) + 2.5(P - 3))/7.59 \times 100] \quad (3)$$

where *K* = soil erodibility factor (ton h MJ<sup>-1</sup> mm<sup>-1</sup>), *OM* is soil organic matter content, *M* is product of the primary particle size fractions, *M* = (%silt + %very fine sand) × (100 – %clay), *S* is soil structure code, *P* is permeability class.

The average soil erodibility for each soil type was computed and added to the soil classification shapefile database in ArcView 3.3 software. The shapefile was subsequently converted to a 20 m grid of soil erodibility. Areas dominated by Mispah, Hutton and Glenrosa soil forms were assigned a *K* value of 0.070, 0.080 and 0.078, respectively. The soil erodibility ratings are consistent with results obtained by Weaver (1991) and D’Huyvetter (1985) in the Keiskamma catchment. These values are also in line with the soil erosion hazard rating for the soils in the catchment estimated from the South African Binomial Soil Classification System. A soil erodibility map was then developed.

Slope-length (*L*) and slope steepness (*S*)

The effect of topography on erosion is expressed by the *L* and *S* factors in the RUSLE model. The *L* and *S* factors can be computed in GIS using a number of empirical formulae (Mc Cool et al. 1987, 1989; Desmet and Govers 1996). A DEM was used to derive the *L* and *S* parameters using a slope length function available in ArcView SA-TEEC GIS-software. The *L* factor expresses the ratio of rill erosion (caused by flow) to interrill erosion (raindrop impact) to find the loss of soil in relation to the standard plot length of 72.6 ft. Renard et al. (1997) define slope length as the horizontal distance traversed from the origin of overland flow to the point where deposition occurs (a flattened slope) or runoff concentrates into a defined channel. The slope steepness factor (*S*) relates to the effect of the slope gradient on erosion in comparison to the standard plot steepness of 9%. The effect of slope steepness is greater on soil loss compared to slope length.

This study uses a method proposed by Desmet and Govers (1996) to calculate the *L* and *S* factors. Besides interrill and rill erosion, Desmet and Govers (1997) note through field observations that the two-dimensional approach of the RUSLE considers ephemeral gully erosion as a product of flow convergence. In this procedure, the RUSLE is adapted to a two-dimensional landscape in which the upslope length is substituted by the unit contributing area which is defined as the upslope drainage area per unit of contour length. A 20 m DEM created using contours was used to derive topographic variables such as slope length and steepness. The equations developed by Desmet and Govers (1996) were used to calculate *L* and *S* in this study are shown below.



*L* factor:

$$L = \left( \frac{\lambda}{22.13} \right)^m \quad m = \frac{F}{(1+F)} \quad F = \frac{\sin \beta / 0.0896}{3(\sin \beta)^{0.8} + 0.56}$$

$$m = ((\sin([\text{slop}] \times 0.01745) / 0.0896) / (3 \times \text{pow}(\sin([\text{slop}] \times 0.01745), 0.8) + 0.56)) \quad (4)$$

where  $\lambda$  is the slope length along the horizontal projection rather along the sloping surface,  $m$  is the slope length exponent and  $\beta$  is slope angle (%). The *L* factor with upslope drainage contributing area (Desmet and Govers 1996) was computed as:

$$L(i, j) = \frac{(A(i, j) + D^2)^{m+1} - A(i, j)^{m+1}}{x^m D^{m+2} (22.13)^m}$$

$$L = \frac{(\text{pow}([\text{Flowacc}] + 1000, ([m] + 1)) - \text{pow}([\text{Flowacc}], [m] + 1))}{(\text{pow}(100, [m] + 2) \times \text{pow}(22.13, [m]))} \quad (5)$$

where  $A(i, j)$  [ $m$ ] is unit contributing area at the inlet of grid cell,  $D$  is grid spacing and  $x$  is shape correction factor.

The *S* factor was computed thus:

$$S(i, j) = \begin{cases} 10.8 \sin \beta(i, j) + 0.03, \tan \beta(i, j) < 0.09 \\ 16.8 \sin \beta(i, j) - 0.50, \tan \beta(i, j) \geq 0.09 \end{cases} \quad (6)$$

where  $\beta(i, j)$  is the mean slope angle of all sub-grids in the steepest direction (Mc Cool et al. 1987, 1989). Hillslope length  $\lambda$  is calculated as the grid area divided by the total length of streams in the same grid.

#### Cover and management factor (*C*)

The cover and management factor can be estimated in various ways depending on the level of information available. The main factors which control the cover and management factor are canopy cover, surface vegetation, prior land use, mulch cover, surface roughness and soil moisture (Lorentz and Schulze 1995). This wide range of factors is difficult and costly to estimate and often vary considerably during the year. A good estimation of the cover factor which only accounts for the vegetation cover can be derived rapidly from satellite imagery. Satellite imagery acquired during the rain season are more suitable for this application given that soil erosion is most active and vegetation cover is at its peak during this season. The cover factor derived from remote sensing is useful in rural catchments such as the Keiskamma where vegetation is the dominant ground cover. The effect of vegetation cover as a control on soil erosion is well established. Vegetation is regarded as the second most critical factor after topography

(Benkobi et al. 1994; Biesemans et al. 2000). In the RUSLE model, the effect of vegetation cover is incorporated in cover management, the *C* factor.

The application of the Normalized-Difference Vegetation Index (NDVI) derived from remotely sensed images has been proved to be useful in providing an estimate of the vegetation cover management factor. The NDVI (Near Infrared – Red)/(Near Infrared + Red) is a robust vegetation index which has been applied successfully in studies relating to vegetation dynamics. Landsat 5 Thematic Mapper satellite data acquired on 12 December 2006 was

used to derive the NDVI by computing the ratio (Band 4 – Band 3)/(Band 4 + Band 3). The NDVI is highly correlated with the amount of green biomass, and can therefore be applied successfully to provide information relating to the green vegetation variability. Studies by Van der Knijff (1999, 2000) and van Leeuwen (2003, 2005) provide a more refined and reasonable estimation of the *C*-factor using the NDVI.

The Landsat 5 TM image was accurately orthorectified and terrain corrected using satellite orbital math modelling method which applies the Toutin's Low Resolution Model available in the PCI Geomatica orthoengine software (PCI Geomatica 10.3 2009). The Universal Transverse Mercator (UTM) projection in WGS84 was used in the co-registration. A 2.5 m geocoded panchromatic SPOT band for the area was used as the reference image and a 20 m resolution DEM was used to correct for the topographic distortions. The cubic convolution resampling method was used for orthorectification. Rectification errors were less than 0.35 pixels (RMSE). Atmospheric corrections using the Quick Atmospheric Correction algorithm available in ENVI were applied to Landsat 5 TM image to improve the spectral fidelity of the satellite data. Accurate orthorectification of digital satellite imagery ensured that Landsat 5 TM and other ancillary datasets overlaid perfectly. The following equation was used to derive the *C*-factor in this study.

$$C = \exp \left[ -\alpha \frac{\text{NDVI}}{(\beta - \text{NDVI})} \right] \quad (7)$$

where  $\alpha$  and  $\beta$  parameters determine the shape of the NDVI curve. Reasonable results are produced using values of  $\alpha = 2$  and  $\beta = 1$ .

Vegetated areas usual have NDVI values much greater than 0.1 while values less than 0 rarely contain vegetation and relate to non-photosynthetic materials such as water and bare soil. A lower vegetation threshold of 0.05 was set, below which vegetation was envisaged to be absent. The ability of NDVI in estimating vegetation cover was confirmed in the field through extensive ground truthing.

Conservation practice factor (*P*)

The conservation practice *P* factor is an important consideration of the RUSLE model. The support practice factor is defined as the ratio between soil loss with a specific support practice and the corresponding loss with upslope and downslope tillage. Renard and Forster (1983) explain that support practice essentially affects soil erosion through altering the flow pattern, gradients, or direction of surface runoff and by reducing the amount and rate of runoff. Information regarding conservation was obtained through field observations in the Keiskamma using a GPS. Shape files for protected areas which receive high priority in terms of conservation practice were downloaded from the South African Biodiversity Institute website (SANBI 2009). These conservancy zones were assigned a *P* factor of 0.001, reflecting stringent conservation practice in these areas. Field assessments in the rest of the Keiskamma catchment revealed that no significant conservation practices were in place and a *P* factor of 1 was assigned to them. The conservation rating ranges from 0.001 to 1, with a lower *P* value indicating that a more effective conservation practice is in place to curtail soil erosion.

Overgrazing, thicket degradation, and general neglect of the environment in the communal areas are evident in most parts of the catchment. Bennett and Barrett (2007) studied the grazing management systems in some communal areas in the Central Eastern Cape including parts of the Keiskamma catchment and identified three grazing

management systems. The scholars identified the open access system, where there is complete lack of grazing management, the controlled system, where grazing is governed by the community and lastly private grazing, whereby the landowner takes responsibility for the grazing on their private land. Field observations in the catchment indicated that open access and a loose form of community controlled system seem to be operational in the Keiskamma catchment.

Sediment delivery ratios (SDR)

An area based method developed by Vanoni (1975) was used to estimate the sediment delivery ratios (SDR) in the SATEEC GIS system. This method uses a generalized curve derived from experimental work in 300 watersheds. The watershed area at any point in the catchment is computed from the flow accumulation map, which is derived from the DEM pre-processing to compute the *LS* factor (Lim et al. 2005). The power function used to develop the generalized SDR curve is shown below.

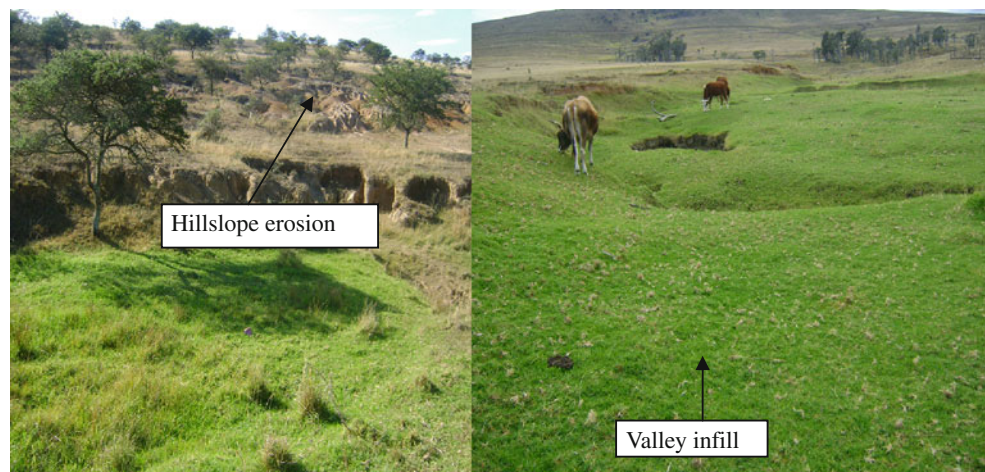
$$SDR = 0.4724A^{-0.125} \tag{8}$$

where, *A* watershed area (km<sup>2</sup>).

Accuracy assessment of soil loss

Model validation was done to ascertain the quality of results produced by the SATEEC model and test the usefulness of the model to predict soil loss. The lack of measured sediment yield data constrained the comparison of simulated sediment yield values with field derived values. An accuracy assessment was thus implemented in this study to only validate the model results in terms of the presence or absence of soil erosion. The Kappa Analysis Tool extension developed by Jenness and Wynnnes (2005)

**Fig. 2** Photographs showing hillslope erosion and valley infill in ephemeral streams



in ArcView 3.3 was used for accuracy assessment. The application is based on the accuracy assessment theory presented by Congalton and Green (1999). The Kappa Analysis method, widely used in remote sensing accuracy assessments is a powerful method used to measure the agreement between predicted and observed phenomena (Jenness and Wynnes 2005).

This study applies Cohen's Kappa to assess the accuracy of the SATEEC soil loss results. Extensive fieldwork was carried in the Keiskamma catchment to randomly identify eroded and non eroded sites and their locations were captured using a GPS. The SATEEC soil loss classes were reclassified into two; low soil loss and high soil loss. The very low and low soil loss classes were reclassified into low soil loss and the moderate to extremely high soil classes were reclassified into the high soil loss classes (after Le Roux et al. 2008). The reclassified soil loss results were then compared with field validated sample points in ArcView 3.3 software.

### Mapping valley infill and erosion features

The valley infill phenomenon is widespread in the degraded ephemeral streams of the central Keiskamma catchment where sediment accumulation is manifest (see Fig. 2). Object oriented classification was used to map valley infill within ephemeral stream channels and erosion features such as gullies. Sediment accumulation in ephemeral stream channels (class 1) can be reliably detected using remote sensing. Other land cover types that were classified include roads (class 2), erosional surfaces (class 3), mixed forest (class 4), sparse and degraded vegetation (class 5). A pan

sharpening algorithm called Principal Component Spectral Sharpening was used for the fusion of Landsat 5 TM and SPOT 5 panchromatic band to enhance the spatial resolution of Landsat 5 TM.

The hybrid fused image possesses both the high spectral resolution of Landsat 5 TM and a high spatial resolution of 2.5 m inherited from the SPOT 5 panchromatic band. Object oriented image classification was achieved by first applying multiresolution segmentation at a scale parameter of 20 before applying the hierarchical classification in Definiens Developer software (Definiens 2009). Layer brightness was used to separate bare areas such as eroded surfaces and roads. The length/width ratio was then used to separate roads from erosion features, as the former are more elongated than the latter. Valley infill and dense vegetation were classified using the NDVI; vegetation vigour within ephemeral channel valley infill is higher than on hillslopes and adjacent areas. The separation of mixed forest from sparse and degraded vegetation was also done using the NDVI thresholding of image objects. The brightness parameter is calculated as follows (Definiens 2009):

$$\bar{c}(v) = \frac{1}{w^B} \sum_{k=1}^K w_K^B \bar{c}_K(v) \quad (9)$$

where  $w_K^B$  = brightness weight of image layer  $k$  with

$$w_K^B = \begin{cases} 0 \\ 1 \end{cases}$$

$K$  = number of image layers  $k$  for calculation;  $w^B$  = sum of brightness weight of all image layers  $k$  used for calculation with

**Fig. 3** Grid surface of the Keiskamma catchment showing the spatial distribution of the rainfall erosivity factor

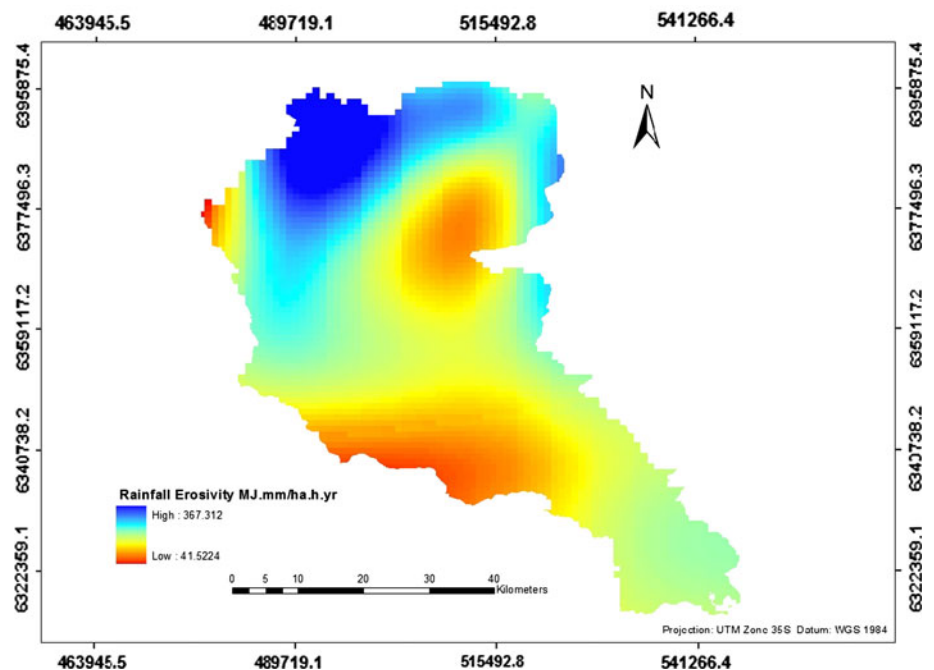




**Fig. 4** Grid surface of the Keiskamma catchment showing the spatial distribution of the soil erodibility factor

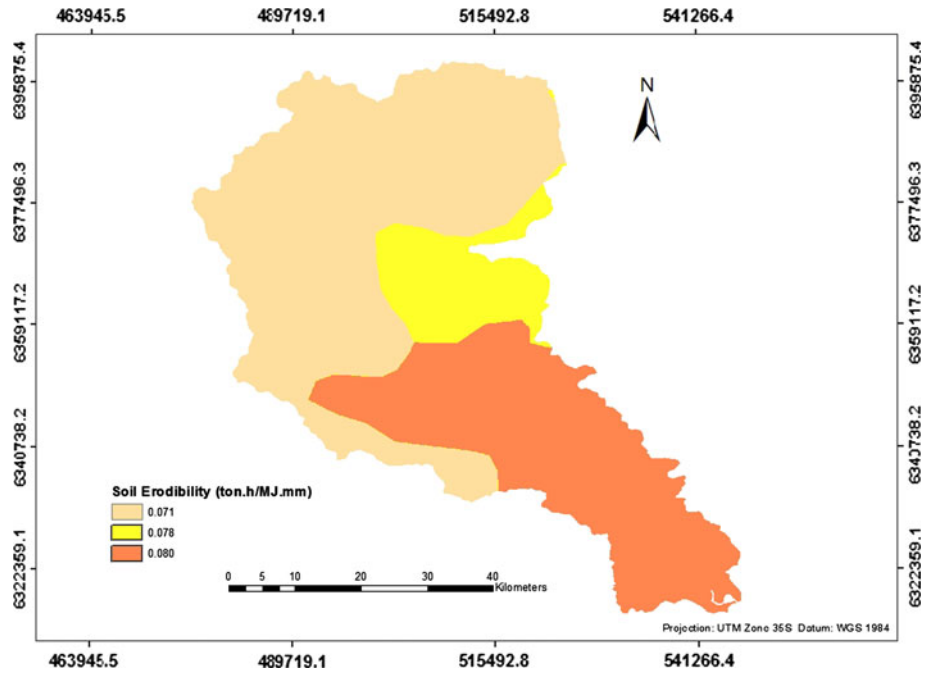
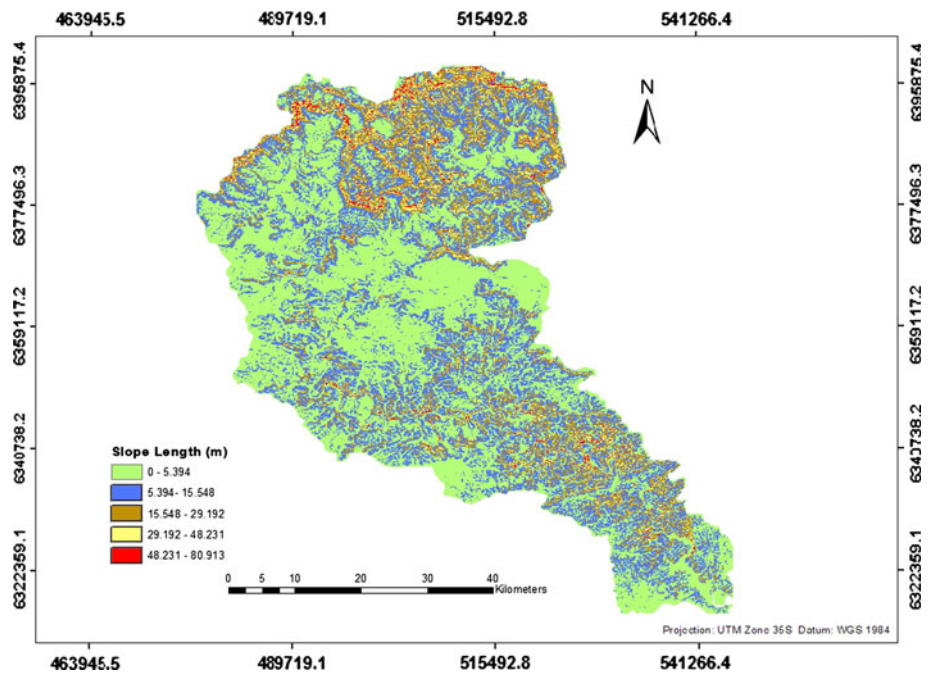


**Fig. 5** Grid surface of the Keiskamma catchment showing the spatial distribution of slope-length



$$W^B = \sum_{k=1}^K W_K^B \tag{9a}$$

where  $\bar{c}_K(v)$  = mean intensity of image layer  $k$  of image object  $v$ ;  $\bar{c}_k^{\min}$  = darkest possible intensity value of image layer  $k$ ;  $\bar{c}_k^{\max}$  = brightest possible intensity value of image layer  $k$ .

Accuracy assessment was done to validate the classification using ground reference data collected using a GPS.

## Results and interpretation

### Soil loss

Results for the RUSLE factors which were computed in this study are presented in Figs. 3, 4, 5, 6 and 7. The SATEEC RUSLE approach effectively illustrates the spatial distribution of soil loss throughout the Keiskamma catchment. The soil loss distributions in the catchment are

**Fig. 6** Grid surface of the Keiskamma catchment showing the spatial distribution of the vegetation cover factor

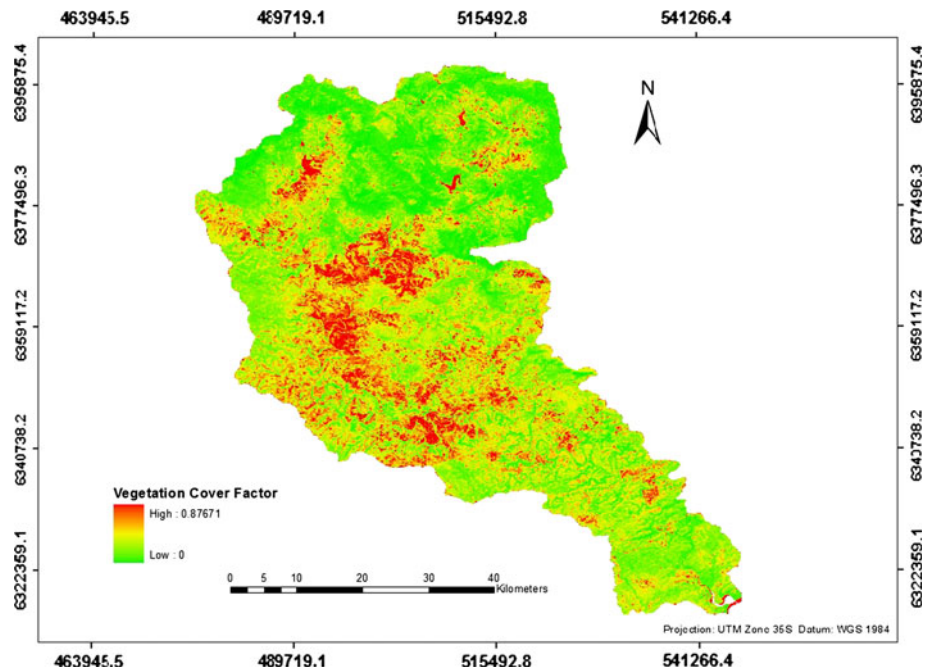
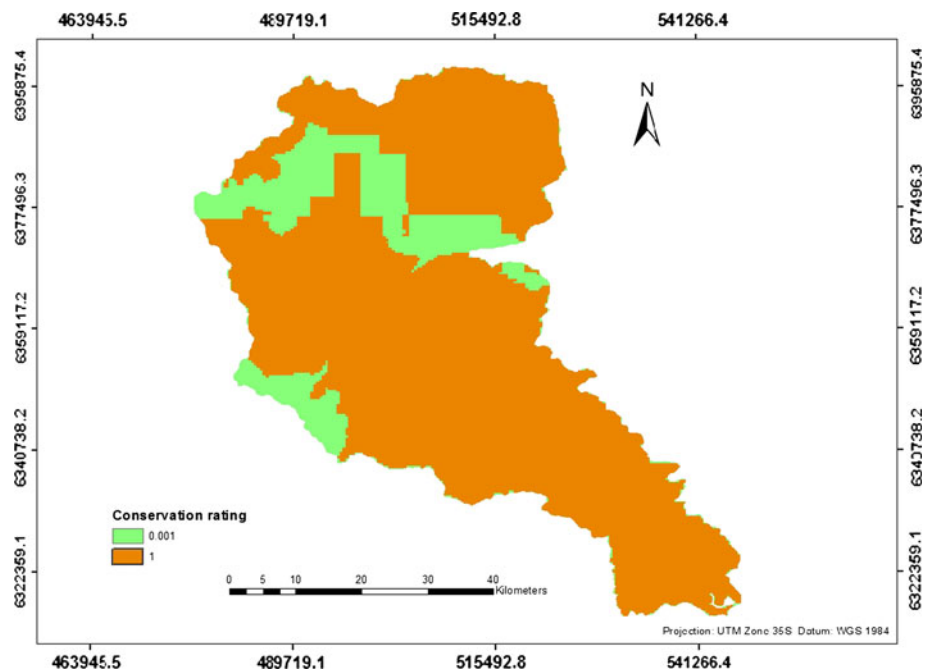


**Fig. 7** Grid surface of the Keiskamma catchment showing the spatial distribution of the conservation practice factor



illustrated by Fig. 8 and the proportions are summarized in Fig. 9. The total soil loss in the Keiskamma catchment is  $9.27 \times 10^6$  ton year<sup>-1</sup> over an area of 257,121 ha. The mean soil loss in the Keiskamma catchment is 36.063 ton ha<sup>-1</sup> year<sup>-1</sup>. Such high sediment yields are not surprising considering the highly dispersive nature of the soils and low vegetation cover in abandoned agricultural fields. Soil erosion is further accelerated by poor rangeland management. Overgrazing and thicket clearance is evident in most communal villages. The protracted history of soil erosion in the Keiskamma catchment is well documented

(Laker 1978; D'Huyvetter 1985). A study by Le Roux et al. (2008) indicates that the average predicted soils loss for South Africa is 12.6 ton ha<sup>-1</sup> year<sup>-1</sup>. Their study further reveals that the Eastern Cape Province has the highest annual soil loss contribution of 28% with a soil loss rate of 25 ton ha<sup>-1</sup> year<sup>-1</sup>. The mean soil loss in the Keiskamma catchment obtained are consistent with the high rates of soil erosion in the Eastern Cape Province if one considers that the former Ciskei and Transkei areas are the most degraded. The greater proportion of the Keiskamma falls within the former Ciskei area.

**Fig. 8** Grid surface of the Keiskamma catchment showing the spatial distribution of soil losses

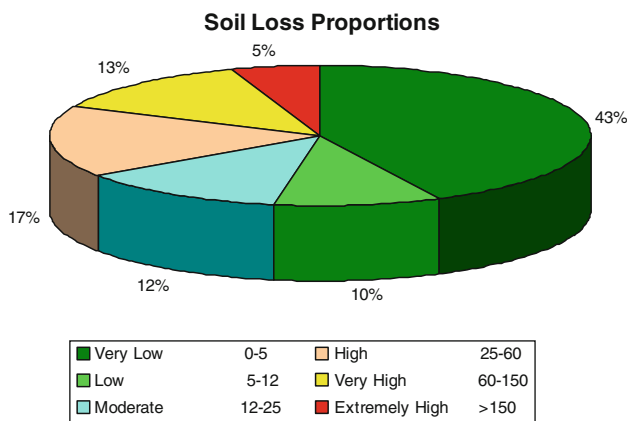
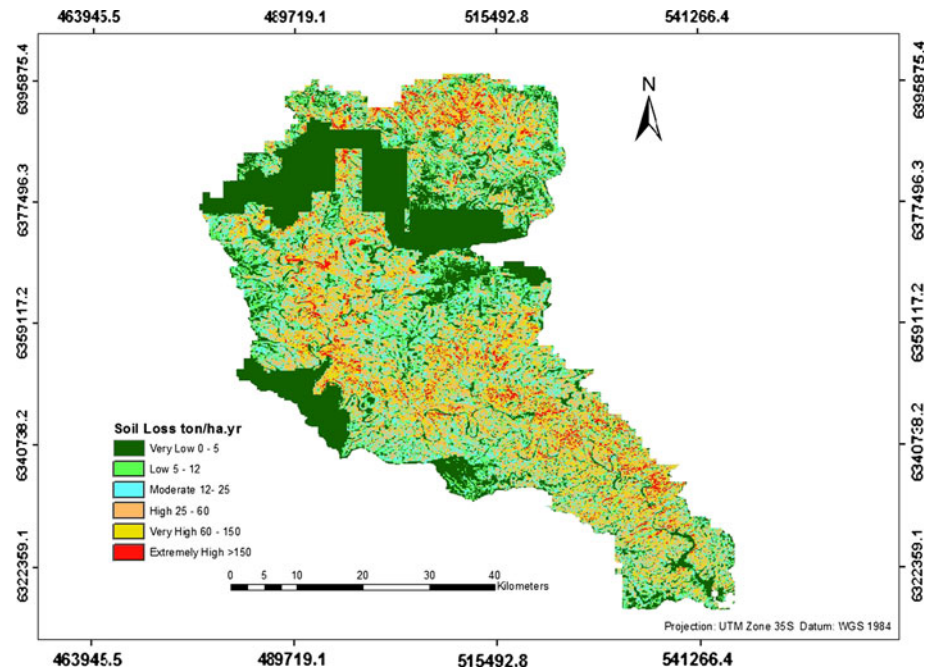


**Fig. 9** Pie chart showing the distribution of soil loss proportions in the Keiskamma catchment

Soil loss tolerances proposed for South Africa range from 3 ton ha<sup>-1</sup> year<sup>-1</sup> for shallow soils and 10 ton ha<sup>-1</sup> year<sup>-1</sup> for deep alluvial soils (McPhee and Smithen 1984). The results indicate that up to 47% of the catchment has soil losses higher than 12 ton ha<sup>-1</sup> year<sup>-1</sup>. It is evident that the rate of soil loss in the Keiskamma catchment is way above sustainable tolerance limits. The remaining proportion of the catchment experiences very low to low soil losses, largely due to the role of vegetation in the form of forest plantations and other conservancy areas.

**Model validation**

The accuracy assessment results for the soil erosion risk assessment are shown in Tables 1, 2, 3 and 4. The proportion error matrix (Table 1) shows the proportional

**Table 1** Proportional error matrix between the re-classed soil loss grid and observed points

Class	No erosion	Erosion	Sum
No erosion	0.256	0.070	0.326
Erosion	0.140	0.535	0.674
SUM	0.395	0.605	1.000

**Table 2** Accuracy report for the accuracy assessment of soil erosion predictions

ID	Producer	User	Specificity	Pred. power	ID class
1	0.647	0.786	0.885	0.793	No erosion
2	0.885	0.793	0.647	0.786	Erosion

**Table 3** Error report for the accuracy assessment of soil erosion predictions

ID	Omission error	Commission error	ID class
1	0.353	0.115	No erosion
2	0.115	0.353	Erosion
Overall	0.209		

classification successes along the diagonal and the proportional misclassifications in the upper and lower triangles. The accuracy report in Table 2 summarizes the producer’s accuracy, user’s accuracy, sensitivity and the specificity of each class (Jenness and Wynnes 2005). The error report shown in Table 3 summarizes the omission and commission error. Table 4 shows the summary overall statistics for the accuracy assessment. An overall

**Table 4** Summary of overall statistics for the soil erosion accuracy assessment

Summary of overall statistics
Overall accuracy/sensitivity: 0.791
Overall misclassification: 0.209
Khat: 0.548
Variance: 0.018
Z: 4.129
P: 0.0000182

accuracy of 79.1% was achieved. Khat is the chance-corrected measure of model accuracy, calculated on the actual agreement between predicted and observed values and the chance agreement between the row and column totals for each classification (Jenness and Wynnes 2005). The Z score of 4.129 and associated P value of 0.0000182 (Table 4) reveal the probability that the SATEEC model performs better than the random chance at predicting the occurrence of erosion on the landscape. It can therefore be concluded that results of the SATEEC model are a good indication of the soil loss distribution in the Keiskamma catchment.

#### Classification of erosion features and valley infill in ephemeral streams

The ability of the object oriented based multiresolution segmentation to delineate soil erosion features such as gullies is illustrated by Fig. 10, where bright white surfaces can be separated from the other land cover types. The object oriented classification results are shown in Fig. 11. Accuracy assessment results (Table 5) for classification of valley infill and erosional surfaces indicate that object oriented classification is an effective means of mapping erosional features and valley infill in ephemeral streams.

An overall accuracy of 92% and kappa coefficient of 0.9 was achieved in the classification. The user's accuracy for valley infill and erosional surfaces was 93.8 and 95.3%, respectively. This classification illustrates the occurrence of valley infill within ephemeral stream channels and the presence of gully erosion on the adjacent hillslopes. These results indicate that both erosion features and sites of sediment deposition can reliably be mapped using object oriented classification.

#### Discussion

The soil loss results show the Keiskamma catchment is experiencing high proportions of soil loss that are above provincial and national averages. The results indicate that the interplay between all the RUSLE factors strongly influence annual soil loss. It is noticeable that areas associated with high rates of soil loss are closely linked to communal settlements where overgrazing and wood harvesting greatly reduce vegetation, leaving the highly erodible soils vulnerable to the effects of soil erosion. Low rates of soil loss are associated with the stringent conservation practices in protected areas such as nature reserves, game parks and forest plantations. Vegetation cover in mega-conservancy areas has a significant curtailing effect on soil loss. Despite the buffering effect of vegetation in the protected zone, high rates of soil loss were noted in its peripheral areas.

The high soil erosion rates obtained in this study might be directly linked to the land use history which entailed land cultivation and abandonment in the 1960s and 1970s. The betterment programme in the 1960s witnessed extensive cultivation above the sustainable topographic slope thresholds in a lot of hillslopes in the area (D'Huyvetter 1985). This was subsequently followed by widespread land

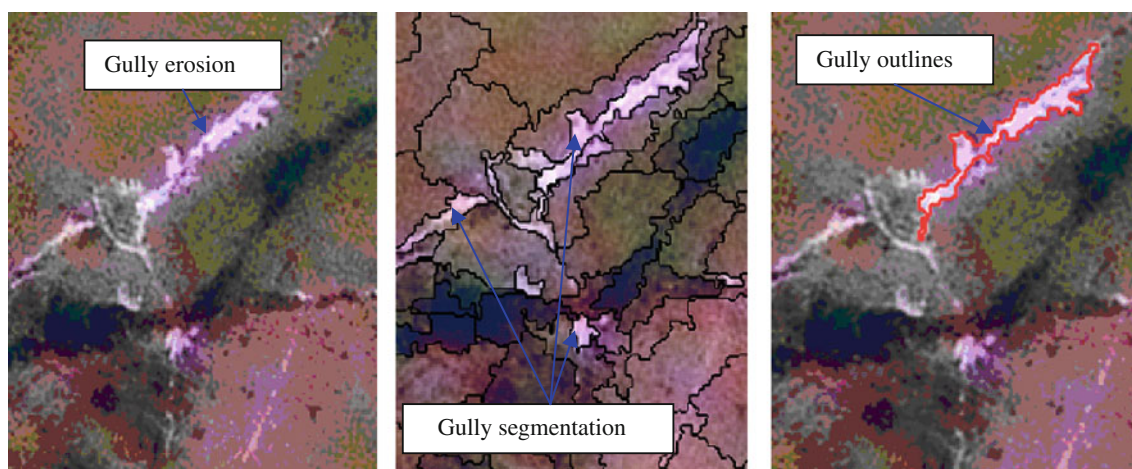


**Fig. 10** Illustration showing the delineation of gullies using multiresolution segmentation on pansharpened satellite imagery



**Fig. 11** Map showing the object oriented classification of valley infill and eroded surfaces in the Keiskamma catchment

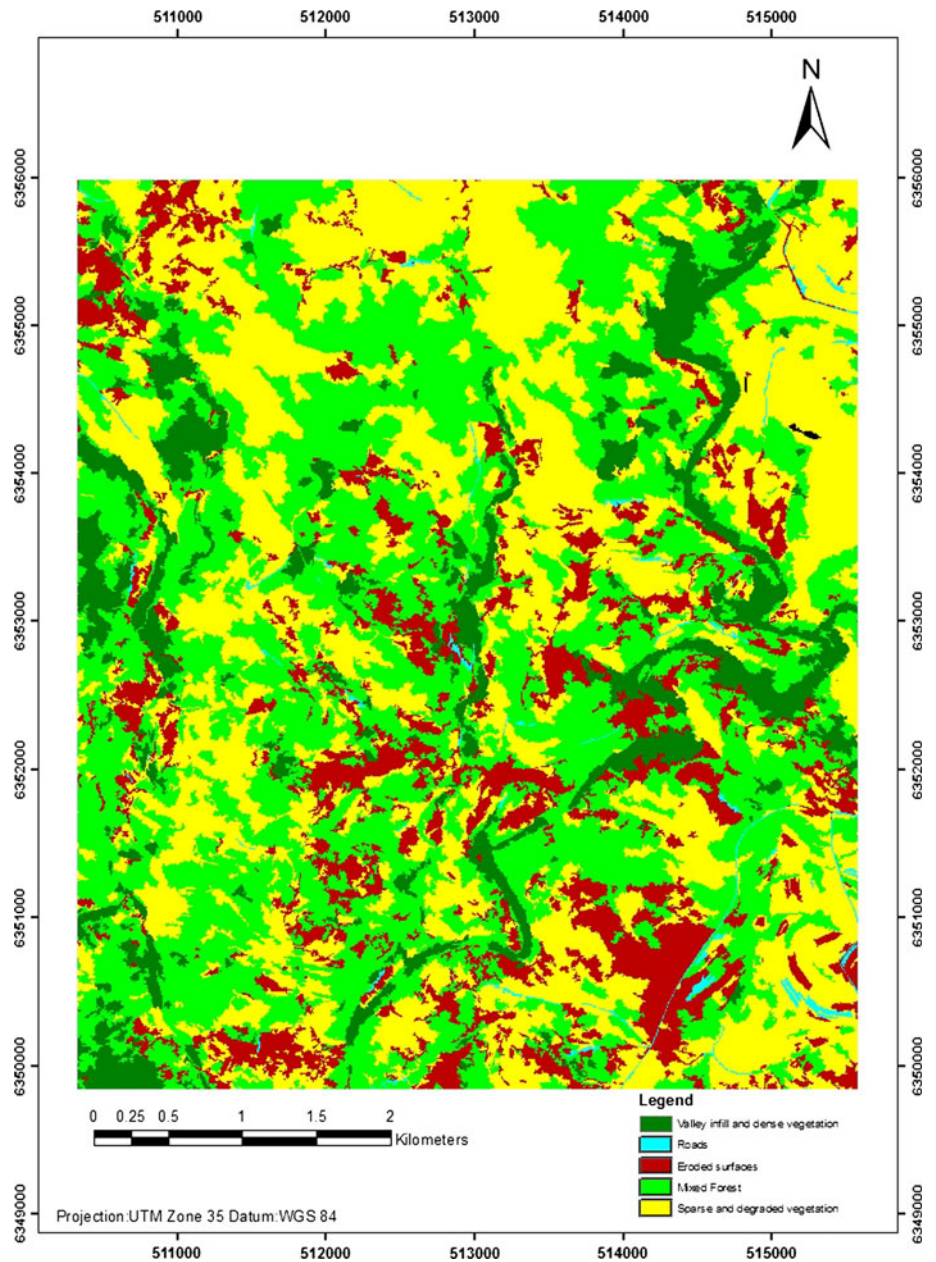


**Table 5** Accuracy assessment of the object oriented land cover classification

Class	Producer's accuracy	User's accuracy	Overall accuracy	Kappa
1	1.000	0.938		
2	0.909	0.952		
3	0.952	0.91		
4	0.700	0.975		
5	0.950	0.905		
			0.921	0.899

1 valley infill, 2 roads, 3 erosional surfaces, 4 mixed forest, 5 degraded forest

abandonment. The low vegetation cover in abandoned agricultural fields exacerbates soil erosion in these areas. The long term effects of cultivation include reduction in aggregate stability through ploughing and destruction of the soil organic content. This increases soil erodibility and renders the soil more vulnerable to soil erosion. These factors are responsible for the high sediment yields computed in this study. Soil erosion is prevalent throughout most communal parts of Keiskamma (Hensley and Laker 1975, 1978; D'Huyvetter 1985). Causes of land degradation in these areas are linked to poor veld management, overgrazing, uncontrolled burning and deforestation associated with harvesting of firewood and medicinal plants.

Injurious cultivation of highly erodible soils also triggered accelerated soil erosion (D'Huyvetter 1985; Laker 1978). Although soil erosion is instigated by a complex interaction of physical, climatic and socio-economic variables, land tenure has been singled out as the most influential feature driving the intensity, rate and extent of degradation in South Africa (Meadows and Hoffman 2002). Marker (1988) indicates that population explosions in the communal areas also contributed to increased soil erosion.

Inaccuracies in the soil loss results obtained in this study are due to limitations linked to some of the parameters used in this study. Hui et al. (2010) indicate that USLE based models tend to overestimate soil loss due to sediment deposition on irregular and long slopes. Slope length segmentations were not accounted for in this study. The absence of the daily rainfall data ( $R$ ) constrained a more accurate estimation of the rainfall erosivity factor. While the SDR equations developed by Vanoni (1975) provides a suitable option if catchment specific coefficients are not available, a more accurate estimation of soil loss can be obtained if catchment-specific coefficient and exponent values of SDR are used. A further limitation of this study arises from the cover and management which only considered vegetation cover. While this approach provided a rapid and cost effective means to compute the cover and management factor, the inclusion of other factors such as prior land use, soil moisture, surface roughness and mulch cover gives a more accurate estimation. That notwithstanding; the parameters used in this study still provide a useful estimation of soil erosion risk in the catchment.

Object oriented classification was able to effectively map erosion surfaces and valley infills prevalent in many parts of the catchment. Vegetation enrichment in the ephemeral streams occurs at the expense of high soil losses from severe gully erosion on the hillslopes. Vegetation growth in ephemeral channels is promoted by enriched sediment feed from hillslopes being deposited into the channels. The highly enriched grass within the main stream channels is now a source of pasture for cattle, sheep and goats. This in turn has led to an inversion of grazing patterns within the catchment, such that grazing is now concentrated within the ephemeral stream channels. This will continue to threaten the ecological health status of the Keiskamma catchment.

## Conclusion

This study reveals the spatial distribution patterns of soil loss and critical sites where erosion and deposition occur within the catchment. The study provides further evidence of alarming soil erosion rates within the catchment as a result of anthropogenic activities. The role of human

activities in controlling vegetation cover and other conservation management initiatives has been noted to have either a negative and positive effect on soil erosion. This aspect is particularly demonstrated by the low soil losses in the protected areas and mega conservancy zones, and the high soil losses in other parts of the catchment such as communal areas with no effective conservation management practices in place. The removal of ground cover through thicket clearance could be curbed by introducing strong communal governance with a robust environmental management framework. Sediment delivery ratios integrated in SATEEC and object oriented classification has effectively mapped the sediment sources and sinks in the Keiskamma catchment. Soil erosion risk information is essential in targeting areas vulnerable to soil erosion for consideration as high priority areas when implementing preventive environmental measures. This study demonstrates that remote sensing and GIS can be used successfully to explain the soil erosion phenomena. Object-oriented classification and GIS modeling are powerful methods for mapping soil erosion patterns and calculating soil losses.

## References

- Angima SD, Stott DE, O'Neill MK, Ong CK, Weesies GA (2003) Soil erosion prediction using RUSLE for central Kenyan highland conditions. *Agric Ecosyst Environ* 97:295–308
- Arnold JG, Srinivasan R, Muttiah RS, Williams JR (1998) Large area hydrologic modeling and assessment part I: model development. *J Am Water Resour Assoc* 34(1):73–89
- Bartsch KP, van Miegroet H, Boettinger J, Dobrowski JP (2002) Using empirical erosion models and GIS to determine erosion risk at Camp Williams. *J Soil Water Conserv* 57:29–37
- Benkobi L, Trlica MJ, Smith JL (1994) Evaluation of a refined surface cover subfactor for use in RUSLE. *J Range Manag* 47:74–78
- Bennett J, Barrett H (2007) Rangeland as a common property resource: contrasting insights from communal areas of central eastern Cape Province, South Africa. *Hum Ecol* 35:97–112
- Bhattarai R, Dutta D (2007) Estimation of soil erosion and sediment yield using GIS at catchment scale. *Water Resour Manag* 21:1635–1647
- Biesemans J, Meirvenne MV, Gabriels D (2000) Extending the RUSLE with the Monte Carlo error propagation technique to predict long-term average off-site sediment accumulation. *J Soil Water Conserv* 55:35–42
- Boggs G, Devonport C, Evans K, Puig P (2001) GIS-based rapid assessment of erosion risk in a small catchment in the wet/dry tropics of Australia. *Land Degrad Dev* 12:417–434
- Congalton RG, Green K (1999) *Assessing the accuracy of remotely sensed data: principles and practice*. Lewis Publishers, Boca Raton
- D'Huyvetter JHH (1985) Determination of threshold slope percentages for the identification and delineation of arable land in Ciskei. M.Sc. Thesis. University of Fort Hare
- Definiens (2009) *Definiens Developer 7: user guide*. Definiens AG, München

- Dennis MF, Rorke MF (1999) The relationship of soil loss by interrill erosion to slope gradient. *Catena* 38:211–222
- Desmet PJJ, Govers G (1997) Two-dimensional modelling of the within-field variation in rill and gully geometry and location related to topography. *Catena* 29(3–4):283–306
- Desmet PJJ, Govers G (1996) A GIS-procedure for automatically calculating the USLE LS-factor on topographically complex landscape units. *J Soil Water Conserv* 51(5):427–433
- DWAF (2004) Amatole-Kei area internal strategic perspective WMA 12. Report. 04 August 2004
- Flanagan DC, Nearing MA (1995) USDA water erosion prediction project: hillslope profile and watershed model documentation. USDA-ARS National Soil Erosion Research Laboratory, West Lafayette
- Flügel WA, Märker M, Moretti S, Rodolfi G (2003) Integrating GIS, remote sensing, ground truthing and modelling approaches for regional erosion classification of semiarid catchments in South Africa and Swaziland. *Hydrol Process* 17:917–928
- Fu BJ, Zhao WW, Chen LD, Zhang QJ, Lü YH, Gulnick H, Poesen J (2005) Assessment of soil erosion at large watershed scale using RUSLE and GIS: a case study in the Loess Plateau of China. *Land Degrad Dev* 16:7
- Garland GG, Hoffman MT, Tod S (2000) Soil degradation. In: Hoffman MT, Todd S, Ntshona Z and Turner S (eds) A national review of land degradation in South Africa. South African National Biodiversity Institute, Pretoria, South Africa, pp 69–107. <http://www.nbi.ac.za/landdeg>
- Hensley M, Laker MC (1975). Land resources of the Ciskei. In: The agricultural potential of the Ciskei—a preliminary report. University of Fort Hare, Alice
- Hensley M, Laker MC (1978) Land resources of the consolidated Ciskei. In: The agricultural potential of the Ciskei. University of Fort Hare, Alice
- Hui L, Xiaoling C, Lim KJ, Xiaobin J, Sagong M (2010) Assessment of soil erosion and sediment yield in Liao watershed, Jiangxi Province, China, Using USLE, GIS, and RS. *J Earth Sci* 21(6):941–953
- Jeness J, Wynne JJ (2005) Cohen's Kappa and classification table metrics 2.0: an ArcView 3x extension for accuracy assessment of spatially explicit models: U.S. Geological Survey Open-File Report OF 2005-1363. USGS
- Kinnell PIA (2000) The effect of slope length on sediment concentrations associated with side-slope erosion. *Soil Sci Soc Am J* 64:1004–1008
- Laker MC (1978) The agricultural potential of the Ciskei. Amended report. University of Fort Hare, Alice
- Lal R (1994) Soil erosion by wind and water: problems and prospects. In: Lal R (ed) Soil erosion research methods, 2nd edn. Soil and Water Conservation Society, St. Lucie Press, pp 1–9
- Lal R (1998) Soil erosion impact on agronomic productivity and environment quality: critical reviews. *Plant Sci* 17:319–464
- Le Roux JJ, Newby TS, Sumner PD (2007) Monitoring soil erosion in South Africa at a regional scale: review and recommendations. *S Afr J Sci* 103(7):7–8
- Le Roux JJ, Morgenthal TL, Malherbe J, Pretorius DJ, Sumner PD (2008) Water erosion prediction at a national scale for South Africa. *Water SA* 34:305–314
- Lim KJ, Choi J, Kim K, Sagong M, Engel BA (2005) GIS-based sediment assessment tool. *CATENA* 64(2005):61–80
- Lorentz SA, Schulze RE (1995) Sediment yield. In: Schulze RE (ed) Hydrology and agrohydrology: a text to accompany the ACRU 3.00 agrohydrological modelling system (report TT69/95, pp. AT16-1 to AT16-32). Water Research Commission, Pretoria
- Marker ME (1988) Soil erosion in a catchment near Alice, Ciskei, Southern Africa. Balkema, Rotterdam
- Märker M, Moretti S, Rodolfi G (2001) Assessment of water erosion processes and dynamics in semiarid regions of southern Africa (KwaZulu/Natal RSA; Swaziland) using the Erosions Response Units Concept. *Geografia Fisica Dinamica Quaternaria* 24:71–83
- McCool DK, Brown LC, Foster GR, Mutchler CK, Meyer LD (1987) Revised slope steepness factor for the Universal Soil Loss Equation. *Trans ASAE* 30:1387–1396
- McCool DK, Foster GR, Mutchler CK, Meyer LD (1989) Revised slope length factor for the Universal Soil Loss Equation. *Trans ASAE* 32:1571–1576
- McPhee PJ, Smithen AA (1984) Applications of USLE in the Republic of South Africa. *Agricultural Engineering in South Africa*
- Meadows ME, Hoffman MT (2002) The nature, extent and causes of land degradation in South Africa: legacy of the past, lessons for the South Africa. University of Cape Town Press, Cape Town
- Millward A, Mersey J (1999) Adapting the RUSLE to model soil erosion potential in a mountainous tropical watershed. *Catena* 38:109–129
- Morgan RPC, Quinton JN, Smith RE, Govers G, Poesen JWA, Auerswald K, Chisci G, Torri D, Styczen ME (1998) The European Soil Erosion Model (EUROSEM): a dynamic approach for predicting sediment transport from fields and small catchments. *Earth Surf Process Landf* 23:527–544
- Nearing MA, Foster GR, Lane LJ, Finkner SC (1989) A process-based soil erosion model for USDA-Water Erosion Prediction Project Technology. *Trans ASAE* 32:1587–1593
- Nyakatawa EZ, Reddy KC, Lemunyon JL (2001) Predicting soil erosion in conservation tillage cotton production systems using the revised universal soil loss equation (RUSLE). *Soil Tillage Res* 57:213–224
- Oldeman LR, Hakkeling RTA, Sombroek WG (1990) World map of the status of human-induced soil degradation: an explanatory note. Revised edn. Wageningen/Nairobi: international soil reference and information. United Nations Environment Programme
- Olderman LR (1994) The global extent of soil degradation. In: Greenland DJ, Saboles T (eds) Soil resilience and sustainable landuse. Commonwealth Agricultural Bureau International, Wallingford
- Onori F, De Bonis P, Grauso S (2006) Soil erosion prediction at the basin scale using the revised universal soil loss equation (RUSLE) in a catchment of Sicily (southern Italy). *Environ Geol* 50:1129–1140
- Park YS, Kim J, Kim NW, Kim SJ, Jeon J, Engel BA, Jang W, Lim K (2010) Development of new R, C and SDR modules for the SATEEC GIS system. *Comput Geosci* 36(2010):726–734
- PCI Geomatica 10.3 (2009) PCI Geomatica Orthoengine manual. PCI Geomatics Inc
- Renard KG, Foster GR (ed) (1983) Soil conservation-principles of erosion by water, Soil Science Society of America. American Society of Agronomy, Madison
- Renard KG, Foster GR, Weesies GA, Porter JP (1991) RUSLE: revised Universal Soil Loss Equation. *J Soil Water Conserv* 46(1):30–33
- Renard KG, Foster GR, Yoder DC, McCool DK (1994) RUSLE revisited: status, questions, answers, and the future. *J Soil Water Conserv* 49(3):213–220
- Renard KG, Foster FG, Weesies GA, McCool DK, Yoder DC (1997) Predicting soil erosion by water: a guide to conservation planning with the revised Universal Soil Loss Equation (RUSLE) (Vol. Handbook #703). US Department of Agriculture, Washington
- SANBI (2009) STEP: conservation priority status. Mega-conservancy networks. <http://bgis.sanbi.org/STEP/priorityStatus.Asp>. Accessed 10 June 2009
- Tanga LV (1992) Rainfall disparities in the Eastern Cape region: the case of Alice and Hogsback (1967 to 1987). Unpublished M.Sc. thesis. University of Fort Hare, Alice, South Africa

- Taruvinga K (2009) Gully mapping using remote sensing: case study in Kwazulu-Natal, South Africa. Masters Thesis. University of Waterloo
- Van der Knijff JM, Jones RJA, Montanarella L (1999) Soil erosion risk assessment in Italy. Joint Research Center of the European Commission, NY
- Van der Knijff JM, Jones RJA, Montanarella AL (2000) Soil erosion risk assessment in Europe. Joint Research Center of the European Commission, NY
- van Leeuwen WJD, Sammons G (2003) Seasonal land degradation risk assessment for Arizona. In: Proceedings of the 30th international symposium on remote sensing of environment, 2003 November 10–14, Honolulu, HI. ISRSE, Tucson
- van Leeuwen WJD, Sammons G (2005) Vegetation dynamics and erosion modeling using remotely sensed data (MODIS) and GIS. In: Tenth biennial USDA forest service remote sensing applications conference, 2004 April 5–9, Salt Lake City, UT. U.S. Department of Agriculture Forest Service Remote Sensing Applications Center, Salt Lake City
- Vanoni VA (1975) Sedimentation engineering, manual and report no.54. American Society of Civil Engineers, New York
- Walling DE (1988) Erosion and sediment yield research—some recent perspectives. *J Hydrol* 100:113–141
- Wang GGG, Fang S, Anderson AB (2003) Mapping multiple variables for predicting soil loss by geostatistical methods with TM images and a slope map. *Photogramm Eng Remote Sens* 69:889–898
- Weaver AvB (1991) The distribution of soil erosion as a function of slope aspect and parent material in Ciskei, Southern Africa. *GeoJournal* 23(1):29–34
- Wischmeier WH, Smith DD (1978) Predicting rainfall erosion losses—a guide to conservation. *Agricultural Handbook* 537. US Department of Agriculture, Washington
- WRC (1995a) Precipitation data for South Africa from the WR90 project. WR90: Surface water resources of South Africa 1990
- WRC (1995b) Geomorphology: soil groups based on 1989 revised broad homogeneous natural regions map-Natal University. WR 90: surface water resources of South Africa 1990